Front. Chem. Sci. Eng. 2018, 12(3): 376–382
https://doi.org/10.1007/s11705-018-1705-z

RESEARCH ARTICLE

Synthesis of hydrophobic carbon nanotubes/reduced graphene oxide composite films by flash light irradiation

Kai Wang (✉)[1*], Jinbo Pang (✉)[2*], Liwei Li[1], Shengzhe Zhou[1], Yuhao Li[1], Tiezhu Zhang[1]

1 College of Automation and Electric Engineering, Qingdao University, Qingdao 266071, China
2 The Leibniz Institute for Solid State and Materials Research Dresden (IFW Dresden), Dresden D-01069, Germany

Abstract Carbon nanotubes/graphene composites have superior mechanical, electrical and electrochemistry properties with carbon nanotubes as a hydrophobicity boosting agent. Their extraordinary hydrophobic performance is highly suitable for electrode applications in lithium ion batteries and supercapacitors which often employ organic electrolytes. Also the hydrophobic features enable the oil enrichment for the crude oil separation from seawater. The ever reported synthesis routes towards such a composite either involve complicated multi-step reactions, e.g., chemical vapor depositions, or lead to insufficient extrusion of carbon nanotubes in the chemical reductions of graphene oxide, e.g., fully embedding between the compact graphene oxide sheets. As a consequence, the formation of standalone carbon nanotubes over graphene sheets remains of high interests. Herein we use the facile flash light irradiation method to induce the reduction of graphene oxides in the presence of carbon nanotubes. Photographs, micrographs, X-ray diffraction, infrared spectroscopy and thermogravimetric analysis all indicate that graphene oxides has been reduced. And the contact angle tests confirm the excellent hydrophobic performances of the synthesized carbon nanotube/reduced graphene oxide composite films. This one-step treatment represents a straightforward and high efficiency way for the reduction of carbon nanotubes/graphene oxides composites.

Keywords carbon nanotubes, graphene composite, flash irradiation method, reduced graphene oxide, contact angles

1 Introduction

Graphene as a 2D material, has shown excellent mechanical [1], electrical [2], optical [3], chemical [4] and electrochemistry [5,6] properties since the pioneering works were reported more than a decade ago. Graphene structures, e.g., monolayer membrane [7–11], thick film [12,13], foam, sponge and vertical walls, aerogel [14–16] and hydrogel have shown great success in the applications of electrode materials in energy storage systems, e.g., lithium ion batteries [17,18] and supercapacitors [19,20]. Very often, the organic electrolytes [21] in the energy storage devices require a hydrophobic electrode for providing sufficient wetting contact and ion exchange [22] or intercalation/deintercalation [23]. Indeed research towards the highly hydrophobic performances remain of great interests [24]. Also the separation of oil from water becomes a focus for solving the environmental problems from crude oil leakage [25]. The oil absorption requires the hydrophobic performances from 3D graphene. However, the intrinsic graphene oxide films have enrichful oxygen containing groups [26,27] and are thus hydrophilic. Therefore, strategies are in high demand for modifying surfaces of graphene oxide to achieve a hydrophobic surface.

Carbon nanotubes, as a super hydrophobic materials, are ideal mixing agents to form graphene composites and boost the hydrophobic performances of 3D graphene [28]. According to the 3D graphene types, the incorporation mechanism of carbon nanotubes can be categorized as chemical vapor deposition and chemical reduction. First, the chemical vapor depositions include an initial step for graphene foam formation over Ni foam and a following step for coating Fe catalyst and carbon nanotube formation. This protocol requires two steps of chemical vapor deposition reactions, which represent a complicated avenue. Second, the chemical reduction [29] refer to the mixing of carbon nanotubes and graphene oxides as

Received November 28, 2017; accepted January 5, 2018

E-mails: wangkai@qdu.edu.cn (Wang K), jinbo.pang@hotmail.com (Pang J)

---

[*] These authors contributed equally to this work.

precursors prior to the hydrogel formation [30] and after a reduction step, the carbon nanotubes/reduced graphene oxide composite is readily formed. In this case, the carbon nanotubes are quite often embedded inside the graphene sheets [31], and are thus difficult to enhance the hydrophobic surface performance. Hence it is highly desirable to find a straightforward way for composite synthesis and facilitate the surface accessibility of the carbon nanotube species.

Here we use a facile flash light irradiation method to induce the reduction of graphene oxide in the carbon nanotubes/graphene oxide composite. The results show that the carbon nanotubes are readily accessible to the surface and an extraordinary hydrophobic performance is thus obtained.

2 Experimental

2.1 Material synthesis

Graphite oxide was synthesized according to the Hummers' method [32] with modification. In details, 5 g of graphite powder (180 mesh, Qingdao Black Dragon Graphite Co. Ltd) and 130 mL concentrated sulfuric acid (98%, Beijing Chemical Works) were mixed into a 1000 mL graduated beaker and mechanically stirred continuously in an ice bath for 2 h. Then 15 g of $KMnO_4$ (Analytic grade, Zhengzhou Third Chemical Reagent Factory) was added slowly, and the resulting solution was stirred for 2 h in the ice bath. Next, the solution was stirred at 35 °C (water bath) for 1 h to further enhance the oxidation of graphite, termed as a mesothermal reaction step. Subsequently, 230 mL of deionized water was added and the diluted suspension was heated up to 98 °C and maintained for 30 min, termed as a hyperthermal reaction stage. After this stage, 400 mL of deionized water was added, and the final solution was centrifuged and rinsed to neutral pH. Eventually, the graphene oxide (GO) suspension formed.

The GO suspension was mixed with 2 g of multi-walled carbon nanotubes (CNTs) and ultrasonicated for 3 h and then a homogeneous black suspension was formed. After the filtering and drying, the CNTs/GO composite film was formed over a filter paper. Then the composite film was irradiated under a camera flash light for 1 h, and eventually became expanded in volume and curved, indicating a complete reduction of graphene oxide (Fig. 1).

2.2 Characterizations

Scanning electron microscopy (SEM) micrographs were collected on a field emission SEM (JEOL S-4800). Surface functional groups were determined with a Fourier transform infrared (FTIR) spectrometer (Bruker Equinox 55). The X-ray diffraction (XRD) curves were captured on a diffractometer named Rigaku D/Max2400 with X-ray sources from Cu Kα 1.54 Å. Raman spectra were collected in Renishaw Raman Spectrometer. Before these measurements, the composite film samples were thermally annealed for degassing for 5 h under vacuum.

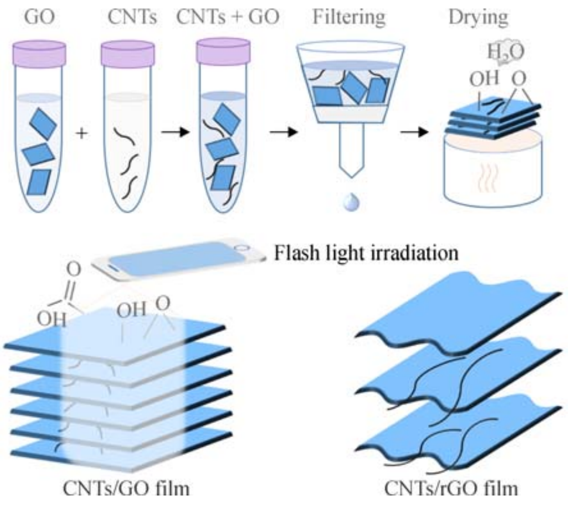

Fig. 1 Illustration of the synthetic route for the CNTs/rGO composite film. rGO, reduced graphene oxide

3 Results and discussion

The carbon nanotubes/graphene oxide composite film has been readily prepared after a typical sonication of the mixture, filtering, and drying according to the synthesis protocol shown in Fig. 1. Before the flash irradiation, the composite film has feature of compact and smooth surfaces which are tailored to three shapes, i.e., square, round and triangle (Fig. 2(a)). After the flash irradiation, the composite film exhibits creases and bumpy surfaces (Fig. 2(b)). Nevertheless, the flash treatment preserves the geometry of the centimeter sized composite film which maintained the complete structure, continuity in morphology and homogeneity.

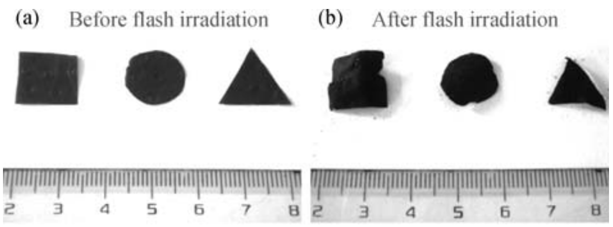

Fig. 2 Photographs of carbon nanotube/graphene oxides composite films: (a) before and (b) after flash light irradiation

From a microscopic view, the carbon nanotubes/graphene oxide composite before the flash irradiation shows compact layer stacking of graphene oxide sheets

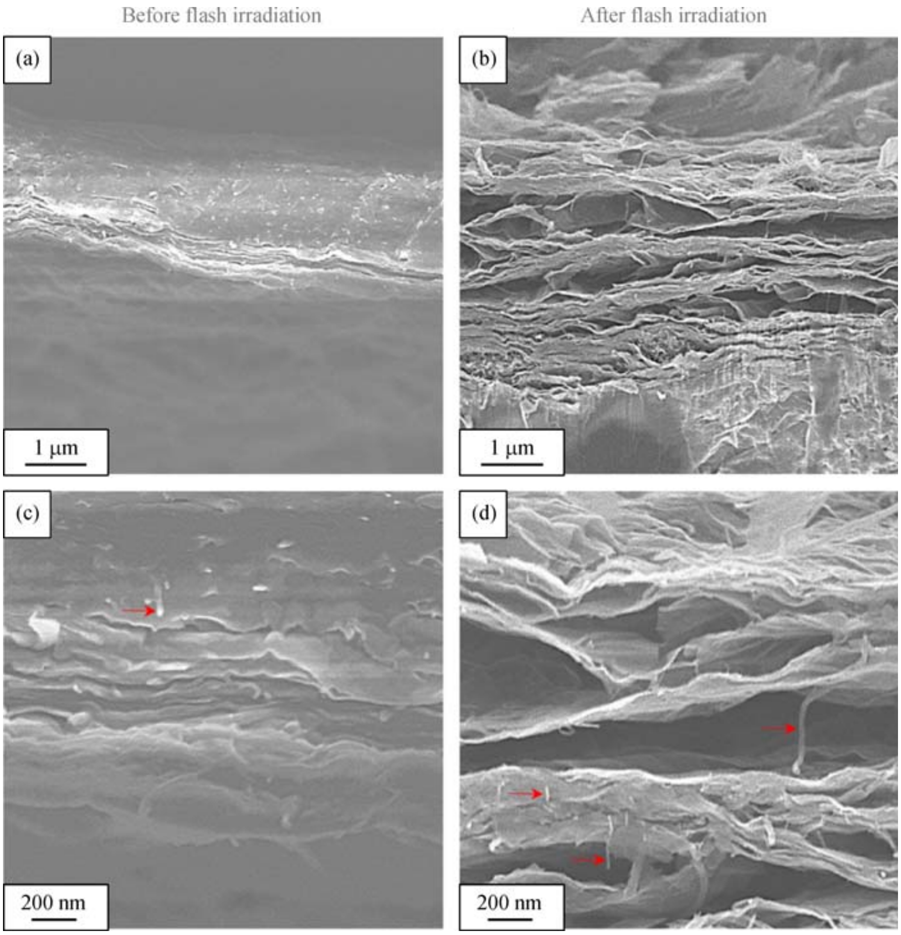

Fig. 3 SEM micrographs of carbon nanotube/graphene oxides composite films: (a) before and (b) after flash light irradiation; (c) and (d) are the magnified micrographs of regions from (a) and (b). Red arrows indicate the carbon nanotubes embedding or standalone in graphene sheets

(Fig. 3(a)). However, after the flash irradiation, the composite shows expansion along the c axis (Fig. 3(b)), which accounts for the total volume enlargement. This volume expansion renders the flash treated sample much larger accessible surface areas and the accessibility of carbon nanotubes compared with the pristine sample (Figs. 3(c) and 3(d)). Moreover, the carbon nanotubes are well distributed and homogeneously dispersed in the flash treated sample, especially individual carbon nanotubes between the graphene sheets (indicated by red arrows in Fig. 3(d)), viz. no aggolomation is observed.

Next we investigated the surface chemical groups to determine the reaction nature of the flash treatment. XRD represents a powerful tool to evaluate the evolution of graphene oxides, e.g., XRD shows that (002) planes and (001) basal planes are dominant in graphite and graphene oxides, respectively, whereas (002) planes become dominant again in reduced graphene oxides. In this experiment, graphene oxide shows one individual peak at $2\theta = 11.6°$ and upon CNT mixing, this peak shifts to 9.8°. Based on the Bragg's law $\lambda = 2d_{\mathrm{hkl}}\sin\theta_{\mathrm{hkl}}$, we calculated the basal plane distance with derived equation $d_{\mathrm{hkl}} = 0.5\lambda/\sin\theta_{\mathrm{hkl}}$ for graphene oxide (001), viz., the $d_{(001)}$ equals to 0.76 nm for pristine GO species, and 0.90 nm for CNT/GO samples. The slightly larger spacing in CNT/GO indicates the well dispersed incorporation of CNT between GO sheets in an embedding way. However, this peak disappears in the flash treated samples and instead a peak at $2\theta = 26.0^{\mathrm{o}}$ becomes the dominant peak (Fig. 4). This could be due to the few layered stacking of graphenes or the multi walled stacking of carbon nanotubes, i.e., $d_{(002)} = 0.34$ nm. This also indicates that the elimination of the graphene oxide phases and the formation of a new graphene like phase. These diffraction data agree well with previous reports, i.e., the graphene oxide has a characteristic peak at $2\theta = 11°$ at (001) direction [33] and the reduced graphene oxide shows at $2\theta = 26°$ at (002) direction [34]. In addition, carbon nanotubes, the composite of carbon nanotubes and graphene oxides, and the flash treated composite all show a peak at $2\theta = 26°$, which is assigned to the sp^2 hybridized carbon structure.

FTIR spectroscopy provides the precise information

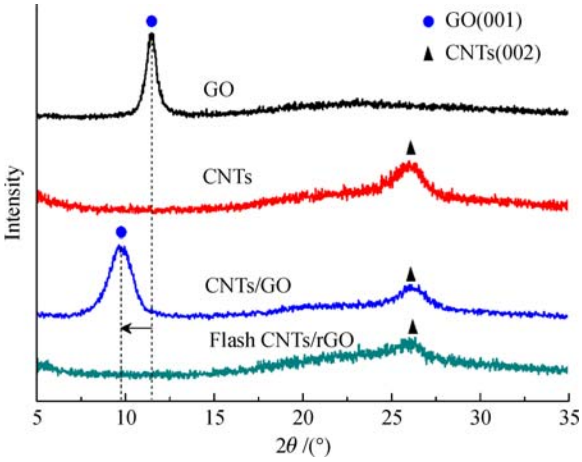

Fig. 4 XRD profiles of GO, CNTs, CNTs/GO, and CNTs/rGO

about surface functional groups with the various molecular vibration modes. For a C = C bond, the stretching mode is at 1600 cm^{-1} [35]. There are three specific vibrational modes of oxygen-containing groups [36]: 1350 cm^{-1} for C–O–H, 1050 cm^{-1} for C–O, and 1728 cm^{-1} for C = O. In this work, graphene oxide and its carbon nanotube composite both show the C–C bond (Fig. 5). Compared with the composite film before and after flash irradiation, the flash treated sample shows elimination of C = O and C–O bonds, which confirmed the successful conversion of graphene. In addition, the graphene and carbon nanotubes have been combined perfectly without any oxygen groups, which account for the boosting in the hydrophobic performances.

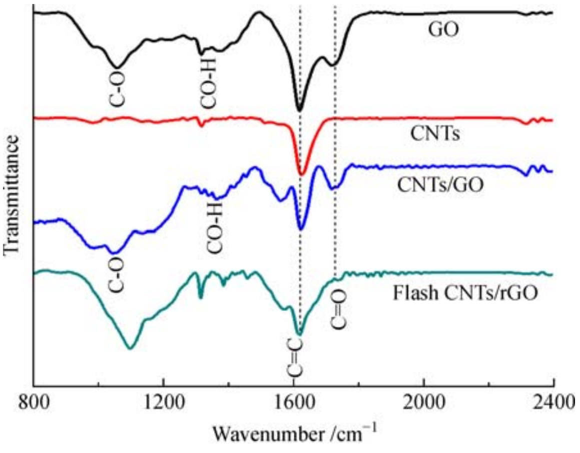

Fig. 5 FTIR spectra of GO, CNTs, CNTs/GO, and CNTs/rGO

A select of the topmost of the flash treated composite film shows a typical wrinkled structure of a reduced graphene oxide which possesses a few layers of graphene (Fig. 6(a)). Indeed the morphology of the flash treated composite sample become crumpled or curved, which greatly enlarge the surface area. Then, a browsing towards the bulk side shows the tight combination between carbon nanotubes and graphene sheets (Fig. 6(b)). This further confirmed the complete reduction of the flash treated composite sample.

Thermogravimetric analysis represents a useful tool that can determine different carbon species with continuously increasing combustion temperature. There are specific combustion temperatures for amorphous carbon, surface groups on graphene oxides, pristine graphene, and carbon nanotubes [37]. The thermogravimetric analysis are shown in Fig. 7 for of the individual carbon nanotubes and graphene oxides, as well as their composites before and after flash treatments. At 84 °C, the gravimetric weight losses are from the liberation of water. At 233–247 °C, the carbon containing surface groups combust and vanish. At 481–497 °C, the graphene burns out. At 581–612 °C, the carbon nanotubes burn and disappear. Compared the flash treated composite with untreated composite, the latter shows the combustion weight loss of surface functional groups while the former does not, indicating the successful removal of these functional groups in the flash induced reduction process.

Therefore, XRD, FTIR, and thermogravimetric analysis all indicate that the flash treatment is a reduction process of graphene oxides. Now the mechanism illustrated in Fig. 1 turns out to be practical and generalized. With the successful reduction of graphene oxide together with the carbon nanotube dispersion for composite formation in one flash light treatment, we finally investigated the hydrophobic performance of the carbon nanotubes/reduced graphene oxide composite. The pristine carbon nanotubes/graphene oxide composite shows a hydrophilic feature with a contact angle of 45° (Fig. 8(a)). In contrast, the flash treated composite becomes hydrophobic with a contact angle of 120° (Fig. 8(a)). The hydrophobic materials with such a contact angle could be applied in oil-water separation [38] and electrodes [39,40] for electrochemistry systems with organic solvents.

4 Conclusions

A facile protocol has been developed to synthesize the carbon nanotubes/reduced graphene oxide composite in one step by flash light irradiation of the carbon nanotubes/graphene oxides film. The synthesized composite has the complete geometry, morphological continuity and homogeneity, and shows the extraordinary hydrophobic performance. The synthesis process is green and easy to handle without harsh conditions, and may find applications in the preparation of electrodes for supercapacitors and lithium ion batteries. The future tuning of the exposure time for flash treatment would lead to the fundamental understanding of evolution kinetics of graphene oxides, e.g., the

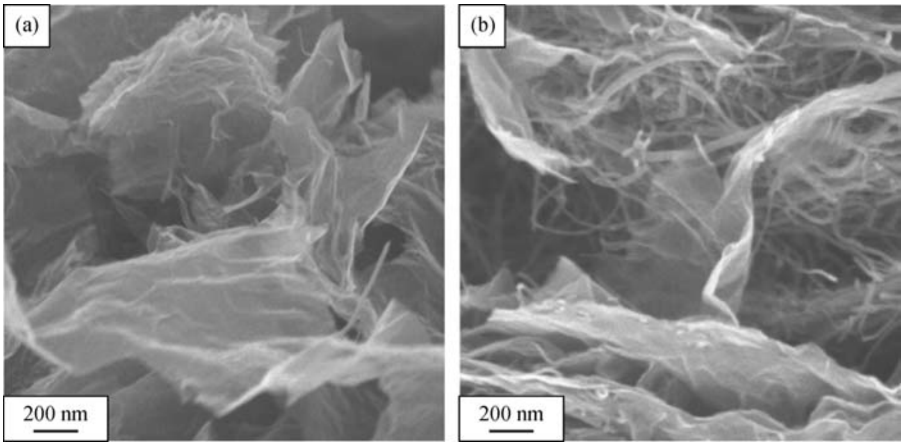

Fig. 6 High magnification SEM micrographs of CNTs/rGO. (a) Standalone graphene sheets with wrinkles; (b) carbon nanotubes standing over the graphene sheets

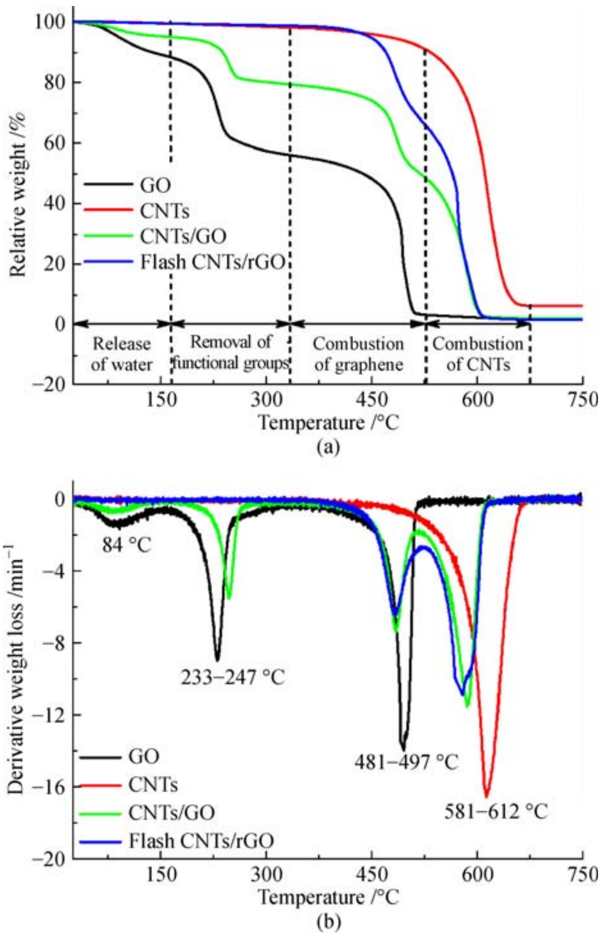

Fig. 7 Thermogravimetric analysis of GO, CNTs, CNTs/GO, and CNTs/rGO

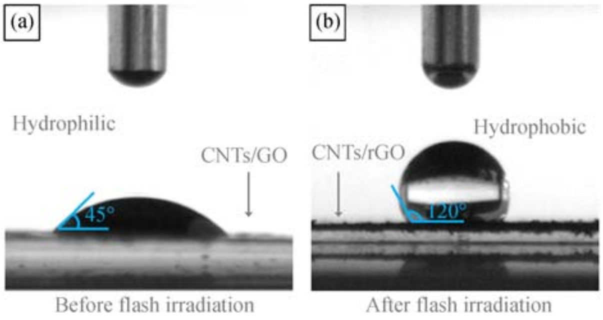

Fig. 8 Contact angles and wetting test of microscopic water droplet on (a) CNTs/GO and (b) CNTs/rGO surfaces

contents of remaining oxygen groups, through thermogravimetric analysis. This is important for providing a general pattern for such a flash induced reduction of graphene oxides. Also, another opportunity falls in the optimization of the ratio of carbon nanotubes in the composites, which may hold promise in further achieving a superhydrophobic performance.

Acknowledgements The work was supported by the Qingdao postdoctoral fund (No. 2015118) and Key research and development plan of Shandong Province (No. 2017GGX50114).

References

1. Mathew J P, Patel R N, Borah A, Vijay R, Deshmukh M M. Dynamical strong coupling and parametric amplification of mechanical modes of graphene drums. Nature Nanotechnology, 2016, 11(9): 747–751
2. Levendorf M P, Kim C J, Brown L, Huang P Y, Havener R W, Muller D A, Park J. Graphene and boron nitride lateral heterostructures for atomically thin circuitry. Nature, 2012, 488 (7413): 627–632
3. Nien L W, Chen K, Dao T D, Ishii S, Hsueh C H, Nagao T. Far-field and near-field monitoring of hybridized optical modes from Au nanoprisms suspended on a graphene/Si nanopillar array. Nanoscale, 2017, 9(43): 16950–16959
4. Johns J E, Hersam M C. Atomic covalent functionalization of

graphene. Accounts of Chemical Research, 2013, 46(1): 77–86

5. Wang K, Li L W, Zhang T Z, Liu Z F. Nitrogen-doped graphene for supercapacitor with long-term electrochemical stability. Energy, 2014, 70: 612–617
6. Lu Y, Zhang N, Jiang S, Zhang Y, Zhou M, Tao Z, Archer L A, Chen J. High-capacity and ultrafast Na-ion storage of a self-supported 3D porous antimony persulfide-graphene foam architecture. Nano Letters, 2017, 17(6): 3668–3674
7. Pang J, Mendes R G, Wrobel P S, Wlodarski M D, Ta H Q, Zhao L, Giebeler L, Trzebicka B, Gemming T, Fu L, et al. Self-terminating confinement approach for large-area uniform monolayer graphene directly over Si/SiO$_x$ by chemical vapor deposition. ACS Nano, 2017, 11(2): 1946–1956
8. Rummeli M H, Gorantla S, Bachmatiuk A, Phieler J, Geissler N, Ibrahim I, Pang J B, Eckert J. On the role of vapor trapping for chemical vapor deposition (CVD) grown graphene over copper. Chemistry of Materials, 2013, 25(24): 4861–4866
9. Pang J, Bachmatiuk A, Ibrahim I, Fu L, Placha D, Martynkova G S, Trzebicka B, Gemming T, Eckert J, Rümmeli M H. CVD growth of 1D and 2D sp^2 carbon nanomaterials. Journal of Materials Science, 2015, 51(2): 640–667
10. Pang J B, Bachmatiuk A, Fu L, Yan C L, Zeng M Q, Wang J, Trzebicka B, Gemming T, Eckert J, Rummeli M H. Oxidation as a means to remove surface contaminants on Cu foil prior to graphene growth by chemical vapor deposition. Journal of Physical Chemistry C, 2015, 119(23): 13363–13368
11. Pang J B, Bachmatiuk A, Fu L, Mendes R G, Libera M, Placha D, Martynkova G S, Trzebicka B, Gemming T, Eckert J, et al. Direct synthesis of graphene from adsorbed organic solvent molecules over copper. RSC Advances, 2015, 5(75): 60884–60891
12. Wang K, Li L W, Xue W, Zhou S Z, Lan Y, Zhang H W, Sui Z Q. Electrodeposition synthesis of PANI/MnO$_2$/graphene composite materials and its electrochemical performance. International Journal of Electrochemical Science, 2017, 12(9): 8306–8314
13. Zhang L, Ji B C, Wang K, Song J Y. Synthesis of nitrogen-doped graphene via solid microwave method. Materials Science and Engineering B, 2014, 185: 129–133
14. Hu H, Zhao Z, Wan W, Gogotsi Y, Qiu J. Ultralight and highly compressible graphene aerogels. Advanced Materials, 2013, 25(15): 2219–2223
15. Hu H, Zhao Z B, Gogotsi Y, Qiu J S. Compressible carbon nanotube-graphene hybrid aerogels with superhydrophobicity and superoleophilicity for oil sorption. Environmental Science & Technology Letters, 2014, 1(3): 214–220
16. Hu H, Zhao Z B, Zhang R, Bin Y Z, Qiu J S. Polymer casting of ultralight graphene aerogels for the production of conductive nanocomposites with low filling content. Journal of Materials Chemistry. A, Materials for Energy and Sustainability, 2014, 2(11): 3756–3760
17. Yu L, Hu H, Wu H B, Lou X W. Complex hollow nanostructures: Synthesis and energy-related applications. Advanced Materials, 2017, 29(15): 1604563
18. Hu H, Zhang J, Guan B, Lou X W. Unusual formation of CoSe@carbon nanoboxes, which have an inhomogeneous shell, for efficient lithium storage. Angewandte Chemie International Edition, 2016, 55(33): 9514–9518
19. Wang K, Zhang L, Ji B C, Yuan J L. The thermal analysis on the stackable supercapacitor. Energy, 2013, 59: 440–444
20. Wang K, Li L, Yin H, Zhang T, Wan W. Thermal modelling analysis of spiral wound supercapacitor under constant-current cycling. PLoS One, 2015, 10(10): e0138672
21. Lin K X, Gomez-Bombarelli R, Beh E S, Tong L C, Chen Q, Valle A, Aspuru-Guzik A, Aziz M J, Gordon R G. A redox-flow battery with an alloxazine-based organic electrolyte. Nature Energy, 2016, 1 (9): 16102
22. Zhou H H, Peng Y T, Wu H B, Sun F, Yu H, Liu F, Xu Q J, Lu Y F. Fluorine-rich nanoporous carbon with enhanced surface affinity in organic electrolyte for high-performance supercapacitors. Nano Energy, 2016, 21: 80–89
23. Markevich E, Salitra G, Chesneau F, Schmidt M, Aurbach D. Very stable lithium metal stripping-plating at a high rate and high areal capacity in fluoroethylene carbonate-based organic electrolyte solution. ACS Energy Letters, 2017, 2(6): 1321–1326
24. Li Y, Luong D X, Zhang J, Tarkunde Y R, Kittrell C, Sargunaraj F, Ji Y, Arnusch C J, Tour J M. Laser-induced graphene in controlled atmospheres: From superhydrophilic to superhydrophobic surfaces. Advanced Materials, 2017, 29(27): 1700496
25. Feng C, Yi Z, She F, Gao W, Peng Z, Garvey C J, Dumee L F, Kong L. Superhydrophobic and superoleophilic micro-wrinkled reduced graphene oxide as a highly portable and recyclable oil sorbent. ACS Applied Materials & Interfaces, 2016, 8(15): 9977–9985
26. Zhang Y X, Zhang H, Wang Y K, Wu H X, Zeng B, Zhang Y J, Tian Q W, Yang S P. Hydrophilic graphene oxide/bismuth selenide nanocomposites for CT imaging, photoacoustic imaging, and photothermal therapy. Journal of Materials Chemistry. B, Materials for Biology and Medicine, 2017, 5(9): 1846–1855
27. Sakai N, Kamanaka K, Sasaki T. Modulation of photochemical activity of titania nanosheets via heteroassembly with reduced graphene oxide. Enhancement of photoinduced hydrophilic conversion properties. Journal of Physical Chemistry C, 2016, 120(42): 23944–23950
28. Wang W Y, Liu P L, Wu K, Tan S, Li W S, Yang Y Q. Preparation of hydrophobic reduced graphene oxide supported Ni-B-P-O and Co-B-P-O catalysts and their high hydrodeoxygenation activities. Green Chemistry, 2016, 18(4): 984–988
29. Jeon Y, Han X G, Fu K, Dai J Q, Kim J H, Hu L B, Song T, Paik U. Flash-induced reduced graphene oxide as a Sn anode host for high performance sodium ion batteries. Journal of Materials Chemistry. A, Materials for Energy and Sustainability, 2016, 4(47): 18306–18313
30. Higgins D, Zamani P, Yu A P, Chen Z W. The application of graphene and its composites in oxygen reduction electrocatalysis: A perspective and review of recent progress. Energy & Environmental Science, 2016, 9(2): 357–390
31. Wan W C, Zhang R Y, Li W, Liu H, Lin Y H, Li L N, Zhou Y. Graphene-carbon nanotube aerogel as an ultra-light, compressible and recyclable highly efficient absorbent for oil and dyes. Environmental Science. Nano, 2016, 3(1): 107–113
32. Chen J, Zhang Y, Zhang M, Yao B W, Li Y R, Huang L, Li C, Shi G Q. Water-enhanced oxidation of graphite to graphene oxide with controlled species of oxygenated groups. Chemical Science (Cam-

bridge), 2016, 7(3): 1874–1881

33. Wang J, Singh B, Maeng S, Joh H I, Kim G H. Assembly of thermally reduced graphene oxide nanostructures by alternating current dielectrophoresis as hydrogen-gas sensors. Applied Physics Letters, 2013, 103(8): 083112
34. Hamid S B A, Teh S J, Lai C W, Perathoner S, Centi G. Applied bias photon-to-current conversion efficiency of ZnO enhanced by hybridization with reduced graphene oxide. Journal of Energy Chemistry, 2017, 26(2): 302–308
35. Jana M, Kumar J S, Khanra P, Samanta P, Koo H, Murmu N C, Kuila T. Superior performance of asymmetric supercapacitor based on reduced graphene oxide-manganese carbonate as positive and sono-chemically reduced graphene oxide as negative electrode materials. Journal of Power Sources, 2016, 303: 222–233
36. Church R B, Hu K W, Magnacca G, Cerruti M. Intercalated species in multilayer graphene oxide: Insights gained from *in situ* FTIR spectroscopy with probe molecule delivery. Journal of Physical Chemistry C, 2016, 120(40): 23207–23211
37. Peng L, Xu Z, Liu Z, Wei Y, Sun H, Li Z, Zhao X, Gao C. An iron-based green approach to 1-h production of single-layer graphene oxide. Nature Communications, 2015, 6(1): 5716
38. Cao N, Lyu Q, Li J, Wang Y, Yang B, Szunerits S, Boukherroub R. Facile synthesis of fluorinated polydopamine/chitosan/reduced graphene oxide composite aerogel for efficient oil/water separation. Chemical Engineering Journal, 2017, 326: 17–28
39. Xiong C, Li T, Dang A, Zhao T, Li H, Lv H. Two-step approach of fabrication of three-dimensional MnO_2-graphene-carbon nanotube hybrid as a binder-free supercapacitor electrode. Journal of Power Sources, 2016, 306: 602–610
40. David L, Bhandavat R, Barrera U, Singh G. Silicon oxycarbide glass-graphene composite paper electrode for long-cycle lithium-ion batteries. Nature Communications, 2016, 7: 10998